EUROFUSION WPPFC-CP(16) 16539

M Laan et al.

Dependence of LIBS spectra on the surface composition and morphology of W/Al coatings

Preprint of Paper to be submitted for publication in Proceedings of 29th Symposium on Fusion Technology (SOFT 2016)

This work has been carried out within the framework of the EUROfusion Consortium and has received funding from the Euratom research and training programme 2014-2018 under grant agreement No 633053. The views and opinions expressed herein do not necessarily reflect those of the European Commission.

Dependence of LIBS spectra on the surface composition and morphology of W/Al coatings

Matti Laan[a], Antti Hakola[b], Peeter Paris[a], Kaarel Piip[a], Märt Aints[a], Indrek Jõgi[a], Jelena Kozlova[a], Hugo Mändar[a], Cristian Lungu[c], Corneliu Porosnicu[c], Eduard Grigore[c], Cristian Ruset[c], Jukka Kolehmainen[d], Sanna Tervakangas[d]

[a]*Institute of Physics, University of Tartu, 50411, Estonia*
[b]*VTT Technical Research Centre of Finland, 02044 VTT*
[c]*National Institute for Lasers, Plasma and Radiation Physics, Bucharest 077125, Romania*
[d] *DIARC-Technology Inc., Finland*

Laser induced breakdown spectroscopy (LIBS) has been applied to study ITER-relevant coatings with different surface morphology and crystallinity. LIBS elemental depth profiles were compared with those obtained by secondary ion mass spectrometry (SIMS). Depending on surface morphology and crystallinity, the laser ablation rate of the coatings changed by an order of magnitude, the highest ablation rate had samples prepared by thermoionic vacuum discharge. The inclusion of aluminum (proxy for beryllium) increased the ablation rate by a factor of > 6. In addition, for W-Al coatings the ablation was non-stoichiometric.

Keywords: ITER relevant coatings, laser induced breakdown spectroscopy (LIBS) diagnostics, ablation rate, surface morphology.

1. Introduction

Laser induced breakdown spectroscopy (LIBS) is a promising tool for remote monitoring of erosion/deposition processes at the first wall of ITER [1]. Proper application of LIBS requires knowing the ablation rates of co-deposited layers on plasma-facing components accurately such that elemental depth profiles for different elements on the layers can be extracted from the recorded LIBS spectra. This goal is, however, complicated by the fact that the ablation rate depends on the composition of the layer as well as on its density, morphology, and the phase structure. Nevertheless, the issue needs to be properly resolved before LIBS can be considered a mature diagnostics for ITER. Results from JET [2] namely indicate that the layers deposited on the first-wall structures can be non-uniform especially in their top sublayer and, as a consequence, significantly increase retention of plasma fuel in them.

To study the effect of layer structure and physical structure on LIBS characteristics, ITER-relevant coatings were produced by different procedures and analyzed by LIBS. The samples were mixed layers consisting of W and Al with Al being a proxy for beryllium.

The LIBS results were compared with those obtained by scanning electron microscopy (SEM), secondary ion mass spectrometry (SIMS), glow-discharge optical emission spectroscopy (GDOES) and X-ray diffraction (XRD) techniques.

2. Experimental

Samples with various mixed W/Al coatings on Mo were used in this study. The coatings were produced by three different techniques: thermoionic vacuum arc (TVA) deposition [3], vacuum arc-discharge (VA) deposition [4], and combined magnetron sputtering and ion implantation (CMSII) [5]. The VA samples contained 100, 90 and 60% of W. D-doped coatings with 100 and 90% of W were produced by TVA method. Pure W coatings were made by the CMSII method. The samples and their main properties have been collected in Table 1. Subscripts in the first column denote the percentage of the W content in the W/Al coatings.

Table 1. List of tested samples

Coating	Procedure	Thickness by SIMS, nm	Ablation rate, nm/shot
W_{100}	VA [3]	2300	≈ 60
W_{90}		1800	≈ 60
W_{60}		2000	≈ 400
W_{100}	TVA [4]	2000	≈ 600
W_{90}		2300	> 800
W_{100}	CMSII [5]	12000	≈ 160

LIBS studies were carried out in vacuum at 10^{-6} mbar residual pressure, more information about the device can be found in [6]. Spectra were excited by a pulsed Nd: YAG laser (532 nm, 8 ns) beam, which was directed onto the sample perpendicular to it. For all sample types the energy of the Gaussian laser beam at the sample surface was 80-90 mJ and the average fluence at the sample surface was Φ = 7 J cm^{-2}. The chosen value was a compromise: on one hand it was close to the minimum value of Φ at which the Mo spectrum could be reliably detectable, on the other hand at this value of Φ the depth

author's email: matti.laan@ut.ee

resolution was still acceptable for especially the TVA samples which according to Table 1 showed the highest ablation rate. Spectra were recorded in the direction perpendicular to the laser beam at 2 mm distance from the sample surface where the intensity of the emission of the expanding plasma plume reached its maximum value. A positive lens with a focal length of 17 cm focal length produced a 1:1 image of the plasma plume at the plane of the entrance slit of a Czerny–Turner spectrometer (MDR-23) coupled with an ICCD camera (Andor iStar DH340T-18F-03). The instrumental halfwidth, FWHM, of the recording system was 0.06 nm. Spectra were recorded in the 385-415 nm wavelength interval. The delay time between the laser pulse and the onset of spectral recording was set to t_d = 120 ns and the width of the recording time-gate to Δt = 400 ns. These resulted in optimal signal-to noise ratio. For each sample, the spectrum as a function of the laser shot number was recorded from five different spots on the sample surface.

A SEM device Helios™ NanoLab 600 (FEI) was applied to characterize the surface morphology. Magnifications from 1000 to 80000 were used. Depth profiles of elements were measured by SIMS. In the analyses, a VG Ionex IX-70S double-focusing magnetic sector instrument with a 5-keV O_2^+ primary ion beam was used. XRD measurements were carried out using SmartLab (Rigaku) diffractometer. The instrumental FWHM was 0.25^0.The wavelength of the X-ray radiation was 1.54 Å (Cu Kα line) and the spectra were measured from 30 to 80 degrees.

3. Results and discussion.

3.1 Results and discussion

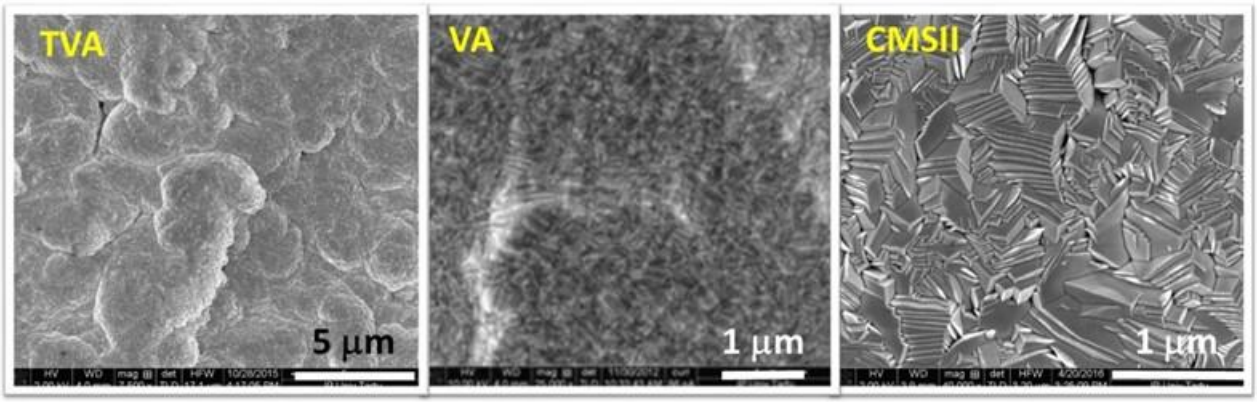

Fig. 1. SEM images of samples produced by different procedures

According to SEM, the morphology of samples prepared by different procedures differ drastically (Fig. 1). TVA samples had few micrometer-size irregularly-formed globular fragments with some deep gaps between them. In contrast, the VA samples showed a flat structure in the sub-micrometer level and the CMSII samples contained a laminar structure micrometer-size aggregates of random orientation.

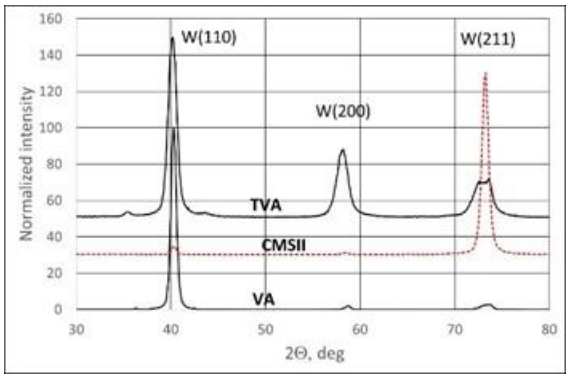

Fig. 2. XRD patterns recorded from samples produced by different procedures.

The XRD patterns in Figure 2 are also different from deposition technique to another. Here, the intensity level of each spectrum has been normalized to that of the highest peak and for better readability the three spectra have been vertically shifted with respect to each other. The peaks around 40^0, 58^0 and 73^0 belong to the tungsten α phase, corresponding to (110), (200) and (211) crystallographic planes. However, the peaks from the substrate Mo at 40.5^0, 58.6^0 and 73.7^0 could also contribute to the patterns. More precise values of angles were obtained by fitting the diffraction peaks using pseudo-Voigt contours, peaks near 73^0 were fitted by two contours. Table 2 contains besides the angles and intensity ratios of patterns peaks the data about standard W and Mo from ICCD PF Cards 01-089-3012 and 00-042-1120.

Table 2. XRD data of the analyzed samples.

Sample	2Θ value, deg			Intensity ratio
TVA	40.16	58.13	72.74*	100:49:34
VA	40.28	58.69	73.15*	100:2.1:4
CMSII	40.32	58.41	73.23	3:0.8:100
Standard W	40.26	58.25	73.18	100:14:24
Standard Mo	40.52	58.61	73.68	100:16:31

* Only one peak is presented in the table, the value of another one coincides with the angle of standard Mo.

Compared with standard W and Mo, the recorded patterns have some remarkable differences. First, peaks of TVA samples have been shifted to smaller angles which could be explained by the presence of residual stress as shown in [7]. Secondly, the intensity ratios for both VA and CMSII samples show the presence of preferential crystallographic planes, whereby VA samples are closest to the standard W. In the case of CMSII samples the

preferential orientation could be related to the laminar structure of the surface (Figure 1).

Besides, peaks of various samples show different halfwidth values. Using the FWHM of dominant peaks of samples and Debye-Scherrer formula, the crystallite size was estimated; the crystallite sizes of TVA, VA and CMSII samples were 14, 30 and 50 nm, respectively.

3.2 Elemental depth profiles by LIBS and SIMS

In the case of TVA and CMSII samples during the first ten laser shots the total emission $I_T = \int I(\lambda)d\lambda$ in the 385-415 nm spectral range remarkably exceeds the corresponding value at larger laser shot numbers, while for VA sample I_T was independent of laser shot number (Fig. 3). According to the samples ablation rate (Table 1) the thicknesses of layers of higher I_T had 1 μm order of magnitude. As increased I_T value indicates more efficient absorption of the laser radiation the surfaces of TVA and CMSII samples are non-uniform and porous down to several μm while the VA samples show a more uniform and compact structure.

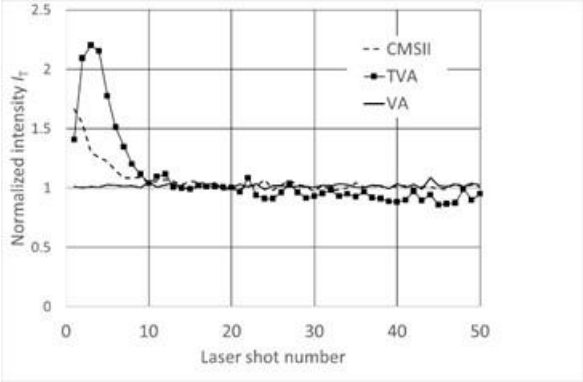

Fig. 3. Total emission I_T as a function of the laser shot number

To extract elemental depth profiles from LIBS measurements, strong spectral lines at 390.2 nm (Mo I), 394.4 (Al I) and 400.9 nm (W I) were selected, the background was subtracted and the integrated intensities were calculated. Multispot averaging of spectra [8] recorded from five different spots on the sample surface, was applied to decrease shot-to-shot intensity fluctuations. In further data processing, the intensities of spectral lines I_{ki} corresponding to the $k \to i$ energy transition were divided by $g_k A_{ki}$ where g_k is the degeneracy of the upper state and A_{ki} is the coefficient of the spontaneous emission. Neglecting self-absorption of spectral lines, the ratio $x_k = I_{ki}/g_k A_{ki}$ is proportional to the population of the upper energy state. For W and Mo the values of upper energy states of the selected spectral lines do not differ much and the partition functions at electron temperatures $T_e \sim 1\ eV$ are almost identical [9]. As a result, for pure W coatings on Mo, $r_{W,Mo} = x_{W,Mo}/(x_W + x_{Mo})$ gives reliable estimations for the relative concentrations of these two elements in the sample. However, for mixed W/Al coatings the situation is more complicated. The value of the partition function of Al differs remarkably from that of W and Mo, meaning that $x_{W,Mo,Al}$, normalized to $(x_W + x_{Mo} + x_{Al})$ do not give reliable values for concentrations but just reflect the relative populations of upper energy states of selected spectral lines.

It appeared that compared to the ordinary normalization to the total plasma emission, the above-described normalization gave in our case a remarkably better smoothing of profiles. As I_T is the sum of the intensities of spectral lines and the continuous spectrum, better smoothing indicates that the correlation between the fluctuations of intensities of spectral lines is remarkably stronger compared with that between the spectral lines and the continuous background radiation [10].

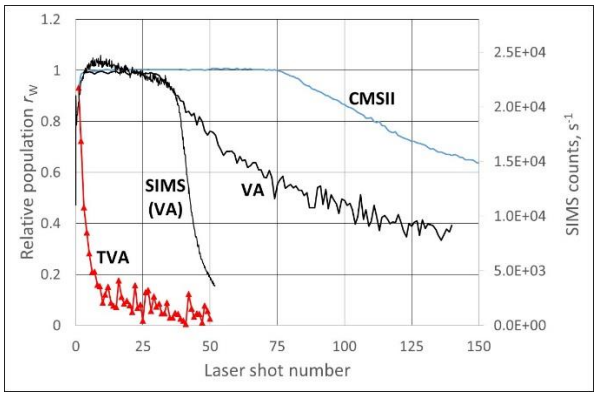

Fig. 4. Elemental depth profiles for W in the case of W_{100} coatings; r_W as a function of laser shot number; SIMS profile of VA sample is fitted with LIBS profile.

Figure 4 shows LIBS depth profiles of W for pure W coatings deposited by different methods. To avoid overloading, in this figure Mo profiles are not presented. Mo becomes detectable when the decay of the W signal starts; as an example, for CMSII sample Mo appears at 75th laser shot.

SIMS profiles show a negligible dependence on the sample type and we used these data for determining the laser ablation rate with the exception of the CMSII coating where GDOES data was applied to extract the true thickness of the sample.

The ablation rates differed by an order of magnitude. According to our experience, after a few laser pulses the surface at the bottom of the laser crater has become smooth independent of its original state. Thus, it is hardly possible to explain the discrepancies in the ablation rate only by roughness-induced differences in the absorption coefficients. A more realistic explanation for the different ablation rates is the different densities of the samples.

Compared with the SIMS profiles, the coating-substrate interface of LIBS profiles is very smooth. It could be explained by the uneven ablation rate along the diameter of the Gaussian laser beam; at the center of the beam the substrate is reached faster than at the edges of the beam. Another explanation is that the ablated (coating) material is redeposited at the bottom of the laser crater and the coating material is detected even then when the original layer is removed.

Fig. 5 shows LIBS depth profiles of different W/Al samples deposited using the VA method. Incorporation of 10% of Al in the coating does not change considerably the ablation rate and the corresponding Mo profile coincides with that of a pure W coating. At the same time instead of being constant within the coating (first 35 laser shots), the ratio r_W/r_{Al} changes gradually (Fig.5B) and grows almost linearly. The highest value of the ratio is ≈ 5. Dissimilarity of Al and W profiles in Fig. 5B is a clear demonstration of non-stoichiometric ablation: because of different values of melting/evaporation temperatures Al is ablated much easier and thus the ratio r_W/r_{Al} changes with the laser shot number [10]. Increasing the Al fraction of the coating to 40% causes a drastic increase of the laser ablation rate (see Mo profiles in Fig. 5A), and the ablation rate becomes comparable to that of the pure W coating produced using TVA. Increased Al content still enhances the ablation non-stoichiometry and now the maximum value of the ratio r_W/r_{Al} was ≈ 1.

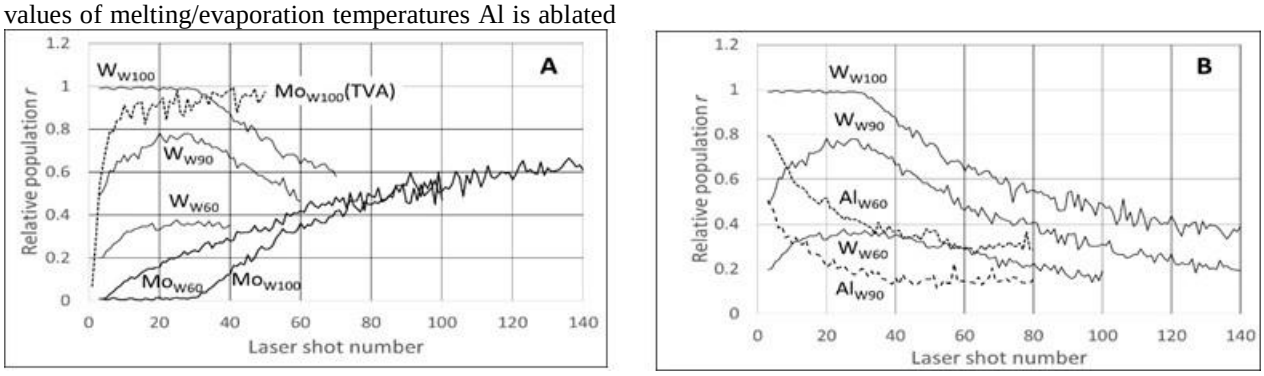

Fig. 5. LIBS profiles for VA samples. Subscripts of data labels give the W content in W/Al coatings. Mo_{W100} profile of the TVA sample is for comparison.

Conclusions

The study brought out a number of facts what should be considered in interpretation of fusion-related LIBS studies.

- Depending on micro-and nanoscale properties of samples the ablation rate of samples with monocomponent coatings could differ by an order of magnitude.
- The surface roughness increases the absorption of the laser radiation. The total emission of the ablated material seems to be an informative source of properties of the porosity and roughness of coatings. .
- A flat coating-surface interface of LIBS elemental profiles could be caused by an uneven ablation rate along the diameter of the Gaussian laser beam as well as by the re-deposition of ablated material into the LIBS crater.
- Drastically different thermal properties of Al and W lead to the ablation non-stoichiometry of Al/W coatings which remarkably complicates the interpretation of results. As Be has more than two-fold higher melting temperature, the effect of non-stoichiometry should be less pronounced.

Acknowledgments

This work has been carried out within the framework of the EUROfusion Consortium and has received funding from the Euratom research and training programme 2014-2018 under grant agreement No 633053. The views and opinions expressed herein do not necessarily reflect those of the European Commission. Work performed under EUROfusion WP PFC.

References

[1] V. Philipps et al, Development of laser-based techniques for in situ characterization of the first wall in ITER and future fusion devices. Nuclear fusion, 53 (2013), 093002

[2] H. Bergsåker et al, Microanalysis of deposited layers in the divertor of JET following operations with carbon wall, Journal of Nuclear Materials 438 (2013) S668–S672

[3] S. Lehto et al, Tungsten coating on JET divertor tiles for erosion/deposition studies, Fusion Engineering and Design (2003) 66- 68 241-245

[4] C P Lungu et al, Beryllium coatings on metals for marker tiles at JET: development of process and characterization of layers, Phys. Scr. T128 (2007) 157–161

[5] C. Ruset et al, Industrial scale 10mm W coating of CFC tiles for ITER-like Wall Project at JET, Fusion Engineering and Design 84 (2009), 1662–1665

[6] A. Lissovski et al, LIBS for tungsten diagnostics in vacuum: Selection of analytes, Journal of Nuclear Materials 463 (2015) 923–926

[7] T.J. Vink et al, Stress, strain and microstructure in thin tungsten films deposited by magnetron sputtering, J. Appl. Phys. 74 (1993) 988-995

[8] P. Paris et al, Determination of elemental depth profiles by multi-spot averaging technique of LIBS spectra, Fusion Engineering and Design 86 (2011) 1125–1128[8]

[9] http://physics.nist.gov/PhysRefData/ASD/levels_form.html

[10] D. W. Hahn and N. Omenetto, Laser-Induced Breakdown Spectroscopy (LIBS), Part II: Review of Instrumental and Methodological Approaches to Material Analysis and Applications to Different Fields, Appl Spectrosc 66 (2021) 347-419